Transient Frequency Response Based Leak Detection in Water Supply Pipeline Systems with Branched and Looped Junctions

Huan-Feng Duan

Department of Civil and Environmental Engineering, The Hong Kong Polytechnic University, Hung Hom, Kowloon, Hong Kong SAR, China (Email: hf.duan@polyu.edu.hk)

ABSTRACT:

The transient frequency response (TFR) method has been widely developed and applied in the literature to identify and detect potential defects such as leakage and blockage in water supply pipe systems. This type of method was found to be efficient, economic and non-intrusive for pipeline condition assessment and diagnosis, but its applications so far are mainly limited to single and simple series pipeline systems. This paper aims to extend the TFR-based leak detection method to more complex pipeline connection situations. The branched and looped pipe junctions are firstly investigated for their influences to the system TFR, so that their effects can be characterized and separated from the effect of other components and potential leakage defects in the system. The leak-induced patterns of transient responses are derived analytically using the transfer matrix method for systems with different pipe junctions, which thereafter are used for the analysis of pipe leakage conditions in the system. The developed method is validated through different numerical experiments in this study. Based on the analytical analysis and numerical results, the applicability and accuracy of the developed TFR-based leak detection method are discussed for practical applications in the paper.

Key words: leak detection; water pipeline system; pipe junction; transient frequency response; transfer matrix; pattern

INTRODUCTION

The problem of potential defects such as leaks and blockages in water supply pipelines has generated great interest for a long time due to its associated cost to industry and health concerns about causing wastes for water and energy resources as well as providing entry points for contaminants (Cheong 1991). In terms of pipe leakage focused in this study, various detection methods have been developed in the past decades and commonly used in water pipeline systems. The most common leak location technique is acoustic analysis. This method involves the use of a special listening device (i.e., geophone) to listen to the sounds emanating from a pipeline. Acoustic analysis relies on the fact that sound emanating from a leak has well-defined characteristics, which enables leak-induced noise to be distinguished from the noise of the mean pipe flows. Infrared thermography technique is another common method and involves the use of infrared imaging to analyze the ground temperature characteristics surrounding water pipes. Other common methods include fluoride testing and tracer gas analysis. While useful, these methods are limited to large leaks and can only work when the operator happens to be in the vicinity of the leak (Wang 2002; Lee 2005). Particularly, the fact that over 30% of water is lost from pipes around the world is a clear testimony that current methods are far from satisfactory (Duan *et al.* 2011).

Recent research activities have intensified the transient-based leak detection methods that utilize the hydraulics of the transient flows to detect leaks in the pipeline (e.g., Liggett & Chen 1994; Brunone 1999; Vítkovský *et al.* 2000; Mpesha *et al.* 2001; Wang *et al.* 2002; Lee *et al.* 2005, 2006; Duan *et al.* 2010, 2011, 2012). The tenet of this kind of methods is that a pressure wave is intentionally injected into the pipeline but its intensity remains in the range of pipe withstanding strengths in all aspects. The system response (e.g., pressure head) is then measured at specified location(s) in the pipeline and analyzed for leak detection (Duan *et al.* 2010). Such transient-based methods have become popular for the advantages of their speed, ability to work online and large operational range (Colombo *et al.* 2009).

A leak in a pipeline system will result in an increased transient damping rate and the creation of new leak reflected signals within the time traces (Tang *et al.* 2000). Many different transient-based leak detection methods have been developed by researchers and applied to water piping systems using information contained within these two effects. The developed leak detection methods vary greatly in their modes of operation, but may be divided into four main categories

according to their utilized different transient information (Duan *et al.* 2010), namely: (1) Transient Wave Reflection (TWR) based method, such as Brunone (1999), Brunone & Ferrante (2001), Meniconi *et al.* (2011), Covas *et al.* (2004); (2) Transient Wave Damping (TWD) based method by Wang *et al.* (2002), Nixon *et al.* (2006); (3) Transient Frequency Response (TFR) based method by Mpesha *et al.* (2001), Ferrante & Brunone (2003), Covas *et al.* (2005), Lee *et al.* (2006), Sattar & Chaudhry (2008), Duan *et al.* (2011, 2012); and (4) Inverse Transient Analysis (ITA) based method studied in Liggett & Chen (1994), Vítkovský *et al.* (2000), Stephens (2008), Covas & Ramos (2010).

While these different types of transient leak detection methods have been proposed and applied to many simple pipe systems in the literature, it was found from many field studies that these methods encounter difficulties in dealing with systems with complex configurations as commonly seen in practical water pipeline systems. Currently, the transient-based methods can only be applied to a pipeline that could be isolated by valves from the rest of the network (Lee 2005; Stephens *et al.* 2004; Stephens 2008). Even then, the solution would fail if this pipeline happens to have changes in diameters (non-uniform). In addition, the effort in going around and isolating pipes is bewildering given that the total length of water supply lines in a modern city attains to an order of 1000 km or more (e.g., about 8000 km in Hong Kong). Therefore, an extension of such transient-based methods to more realistic and complex pipelines is urgently required and practically significant to reduce leakage in urban water supply systems.

In a related work by the author, Duan *et al.* (2011) studied the possibility of leak detection in complex pipeline systems which consist of multiple pipes in series respectively. Both the leak-induced and pipe junctions induced transient effects were investigated analytically and numerically in this study. Using the TFR-based method, an analytical expression was derived for the single leak-induced transient "pattern" in complex series pipelines. The results confirmed that the leak-induced transient behaviors could be separated from those by the connecting junctions of series pipes as long as the original intact (leak-free) complex pipe system is well-defined for its configuration and boundaries and the change extent of pipe diameters at junctions is not too large to violate the linear assumptions made in the analytical derivation. In addition, the analysis indicated that the pipe connecting junctions with different diameters can cause the shifting of the system resonant frequencies but leaks do not, which gives the possibility of separating the leak-induced effect from the junctions. This result was consistent with many

experimental observations in previous work such as Ferrante & Brunone (2003), Lee (2005), and Brunone *et al.* (2008), and thereafter confirmed in relevant studies by the author and his partners (e.g., Meniconi *et al.* 2013; Duan *et al.* 2014; Lee *et al.* 2013).

It is necessary to note that only the cases of single and simple series pipelines are considered in previous studies and for the cases of complex branched and looped pipelines that commonly seen in practical distribution pipelines, an extension of this efficient and non-intrusive method is highly required in both method and application, which is the scope of this study. In this paper, the influences of typical pipe branched and looped junctions to the transient responses are firstly examined by numerical applications. The method and principles for TFR-based leak detection in branched and looped pipeline systems are then derived and developed, which are thereafter applied for different numerical cases. In the end, the results and findings of this study are analyzed and discussed for practical implications in the paper.

MODELS AND METHODs

The one-dimensional (1D) waterhammer model and its equivalent form of transfer matrix in the frequency domain transfer matrix are used in this study, which are described in this section. The classic 1D waterhammer governing equations are expressed as follows (Chaudhry 1987; Wylie *et al*. 1993),

$$\frac{gA}{a^2}\frac{\partial H}{\partial t}+\frac{\partial Q}{\partial x}=0\,, \tag{1}$$

$$\frac{\partial Q}{\partial t}+gA\frac{\partial H}{\partial x}+\frac{f}{2DA}Q|Q|=0\,, \tag{2}$$

where H = pressure head, Q = pipe discharge, A = pipe cross-sectional area, D = pipe diameter, a = acoustic wavespeed, t = time, x = spatial coordinate along pipeline, g = gravitational acceleration, ρ = fluid density and f = pipe friction factor. The method of characteristics is applied to solve the waterhammer model (Chaudhry 1987). Note that only steady friction effect is considered in the analytical derivation and the unsteady friction effect will be included and validated in the numerical simulations.

The frequency domain equivalents of the 1D mass and momentum equations in Eqs. (1) and (2) above can be obtained by applying the linear transfer matrix method for describing the transient system behaviors in the frequency domain (Chaudhry 1987; Lee *et al.* 2006; Duan *et al.* 2010). After linearization and transformation, the result in the frequency domain becomes,

$$\begin{Bmatrix} q \\ h \end{Bmatrix}^2 = \begin{bmatrix} \cosh(\mu l) & \frac{1}{Y}\sinh(\mu l) \\ Y\sinh(\mu l) & \cosh(\mu l) \end{bmatrix} \begin{Bmatrix} q \\ h \end{Bmatrix}^1, \tag{3}$$

or in a matrix form,

$$\boldsymbol{O} = \boldsymbol{U}\boldsymbol{I}, \tag{4}$$

where $\boldsymbol{I}$, $\boldsymbol{O}$, $\boldsymbol{U}$ = input of transient information (e.g., the upstream end), output of transient information (e.g., the downstream end), and the transfer matrix; q, h = transient discharge and pressure head in the frequency domain; l = length of pipe section; the superscripts "1" and "2" represent quantities at the two ends/sides of the pipe section or system element under investigation respectively; μ and Y = propagation factor and impedance coefficient, and,

$$\mu = \frac{\omega}{a}\sqrt{1 - i\frac{gAR}{\omega}}; \quad Y = -\frac{a}{gA}\sqrt{1 + \frac{gAR}{i\omega}}, \tag{5}$$

in which ω = frequency; i = imaginary unit; R = friction related coefficient and $R = fQ_0/gDA^2$ with Q_0 being steady (pre-transient) state discharge. Eq. (3) or Eq. (4) is called transfer matrix equation that represents the modification effect of the given element (e.g., pipeline, junction, and valve) on hydraulic responses from one end/side to the other. With this definition, the frequency response of a whole transient pipe system can then be obtained by multiplying in order the relevant transfer matrices of all the system elements (Lee 2005; Duan *et al.* 2011). This method is used later in this study for deriving the TRF results of the branched and looped pipe systems.

TRANSIENT INFLUENCES OF PIPE JUNCTIONS

Prior to develop the detection methods for complex pipeline systems, it is necessary and also a good start to understand and investigate the impacts of different pipe junctions on the transient responses. For illustration, three test cases of systems with single and uniform pipeline (without junction) and multiple pipes with branched and looped junctions shown in Figs. 1(a) to 1(c) respectively are used herein for comparative study in both the time and frequency domains (denoted as systems no. 1, no. 2, no. 3). Specifically, the main pipelines for these three systems (i.e., from node *a* to node *b*) are assumed to be the same so as to analyze the impacts of junctions on the system transient responses through result comparisons. The details of system settings and parameters are provided in the figure. In each system, the side-discharge valve at the downstream (V_2 in the figure) is used for generating transients and the inline valve (V_1 in the figure) is used for controlling the initial steady state discharge (Q_s) in the system. For simplicity of analysis and

to highlight the transient behaviors (separated from steady state), initially both valves (V_1 and V_2) are fully closed (i.e., Q_s = 0). That is, the transient flows are generated on the basis of initial static flow condition. The effect of initial non-static flow conditions will be included in the analytical and numerical analysis later in this study. In order to provide a preferably large bandwidth of wave injection for transient system analysis (e.g., defect detection), the transients in all test cases are generated by the side-discharge valve with operations of fast closure-open-closure as given in previous studies (e.g., Duan *et al.* 2010, 2011, 2012). The numerical results of transient pressure traces collected at the just upstream of the inline valve are used for analysis.

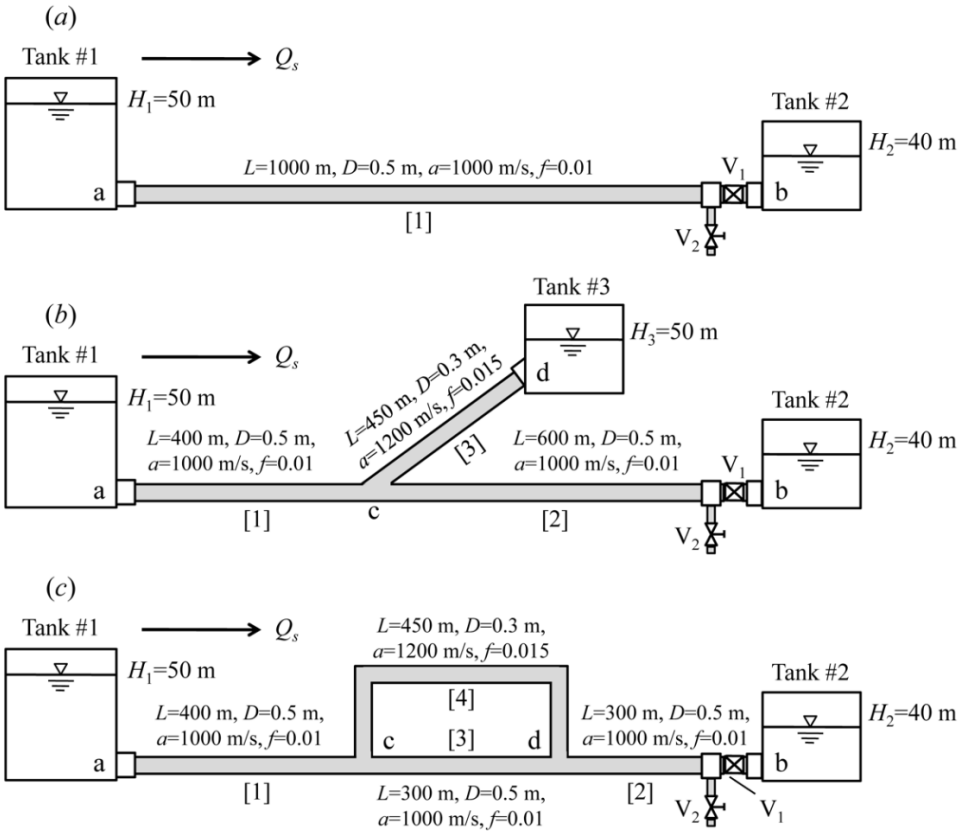

Figure 1: Sketch for test pipeline systems: (a) no. 1: single and uniform pipeline system; (b) no. 2: branched pipeline system; (c) no. 3: looped pipeline system

Time domain transient responses

The obtained transient pressure head responses in the time domain are shown in Fig. 2(a) for the three systems. For comparison, the axial coordinate of the figure is dimensionless time with

regard to wave period of single pipeline case (i.e., $4L_0/a_0$), and the vertical coordinate is normalized by the first peak amplitude of transient head at side-discharge valve (i.e., Joukowsky head, $a_0\Delta V_d/g$ with ΔV_d being the velocity change through the valve operation).

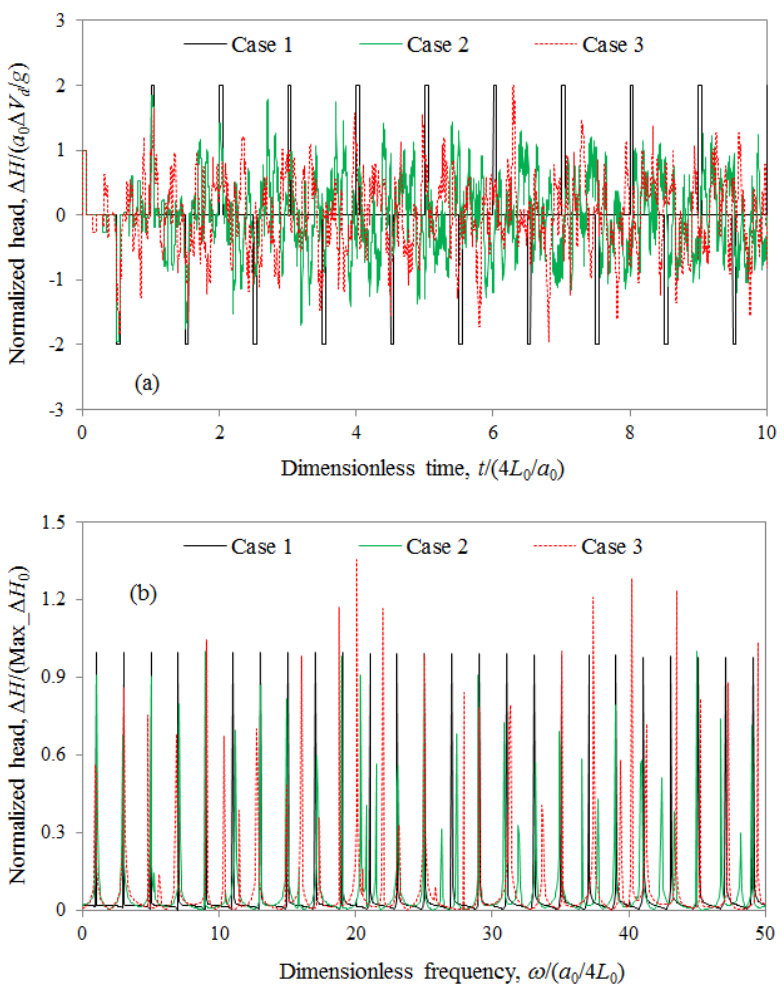

Figure 2: Results of test pipeline systems with/without pipe junctions in: (a) the time domain results; (b) the frequency domain

The results in Fig. 2(a) show clearly the differences of the transient wave histories for the pipeline systems with/without pipe junctions. Particularly, more frequent reflections are caused by the junctions, which results in complex (e.g., non-monotonic) wave amplitude envelope attenuations with time. Moreover, different pipe junctions (e.g., branched and looped junctions here) may induce different extent and frequency of wave reflections from the result comparison

of systems no. 2 and no. 3 in Fig. 2(a). From this regard, it is very difficult to characterize the transient wave behaviors in the time domain for such complex pipeline systems. Therefore, current transient-based time domain methods for pipe leakage detection (i.e., TWR and TWD), which depend mainly on the wave reflection and damping information, may become inapplicable or inaccurate for the pipeline system with complex connection junctions (e.g., series, branched and looped). This result has also been confirmed in the previous study for complex series pipe systems in Duan *et al.* (2011). Based on these findings here and from previous studies, the frequency domain transient response is examined in the following study, with its features used for characterizing and diagnosing relatively complex pipe systems.

Frequency domain transient responses

The transient frequency responses can be obtained from the Fourier transform of the time domain traces in Fig. 2(a), and the results of the three systems are shown in Fig. 2(b) for analysis. Similarly in Fig. 2(a), the axial and vertical coordinates of Fig. 2(b) are dimensionalized by the fundamental frequency ($a_0/4L_0$) and the first peak amplitude of single pipeline case respectively.

As indicated from the time domain results in Fig. 2(a), obvious differences between the results of pipe systems with and without pipe junctions are observed in the frequency domain. With the existence of different pipe junctions, both the resonant frequency shifts and amplitude changes of the transient frequency responses are caused with different extents by the junctions. This result is consistent with various numerical and experimental observations in the previous studies (e.g., Brunone *et al.* 2008; Duan *et al.* 2013, 2014; Duan & Lee 2015). However, compared to time domain results, the influences of pipe junctions to the transient frequency responses are relatively simple and independent for different resonant peaks, which have similar impact complexities that are not superimposed or accumulated with frequency. From this perspective, it might be easier to use the frequency domain results for characterizing the influences of pipe junctions to the transient system responses than the time domain results. Consequently, the TFR-based method is adopted as the investigation tool for the development of leak detection method in the typical branched and looped pipeline systems in this study.

TFR RESULTS FOR DIFFERENT PIPE JUNCTIONS

To develop the leak detection method, it is necessary first to understand and characterize the

difference of the system transient frequency responses under intact (leak-free) and leakage conditions. That is, the leak-induced patterns are required to be explored and derived for the transient frequency responses of complex pipeline systems with pipe connection junctions (Duan *et al.* 2010). Two typical junctions of pipe branch and simple pipe loop shown in Figs. 1(b) and 1(c) are considered in this study. For simplicity and illustration, only the single leakage situation is considered in this study, and for multiple leaks, the similar derivation and analysis procedure can be extended and applied. The main results of TFR for the branched and looped pipe systems are summarized in this section, with the derivation details shown in the appendix in this paper.

For the intact branched pipeline system in Fig. 1(b), the following resonant condition can be obtained by transfer matrix method as given in Eq. (A10) in the appendix,

$$\begin{bmatrix} Y_3 Y_2 \sin(\mu_3 l_3)\cos(\mu_2 l_2)\cos(\mu_1 l_1) \\ -Y_3 Y_1 \sin(\mu_3 l_3)\sin(\mu_2 l_2)\sin(\mu_1 l_1) \\ +Y_2 Y_1 \cos(\mu_3 l_3)\cos(\mu_2 l_2)\sin(\mu_1 l_1) \end{bmatrix} = 0, \tag{6}$$

where subscript numbers are pipe numbers described in Fig. 1(b). This result has been validated and used in previous studies by the author for dead-end side branch detection (e.g., Duan & Lee 2015). Under single pipe leakage condition, after mathematical manipulations and essential simplifications, a general form of the converted transient pressure response in the frequency domain can be obtained as (see Eqs. (A14) through (A16) in the appendix),

$$\hat{h}_{Ln}^{B} = \frac{K_L}{C_n^B}\left[1-\cos\left(2\mu_n x_{Ln} + \phi_n^B\right)\right], \tag{7}$$

where $\hat{h}_{Ln}$ is the converted TFR based on the difference between the intact and leakage situations; n is the number of pipe that the potential leakage is located (n = 1, 2, 3 in this study); x_{Ln} is the distance of leakage location from the upstream end of the pipeline n; K_L is the impendence factor for describing the leakage size; the subscript L is used for quantity for leaking pipe system; the superscript B indicates the quantity for branched pipeline system, and C, ϕ are intact system based known coefficients with their expressions provided in the appendix. The result of Eq. (7) indicates that the leak-induced pattern for transient frequency responses is dependent on the system configuration as well as the location of the leaking pipe section in the system. Moreover, for given intact branched pipeline system, the leak-induced pattern relies only on the potential leak information (location and size), which therefore can be used inversely to identify and detect pipe leakage in the system.

Similarly, for the simple looped pipeline system in Fig. 1(c), the leak-induced patterns for different leaking conditions can be derived and expressed as follows (see Eqs. (B11) and (B12) in the appendix):

$$\hat{h}_{Ln}^{O} = \frac{K_L}{C_n^O}\left[R_n^O + \sqrt{\left(S_n^O\right)^2 + \left(T_n^O\right)^2}\,\sin\left(\mu_n l_n - 2\mu_n x_{Ln} + \phi_n^O\right)\right], \tag{8}$$

where the superscript O indicates the quantities obtained for the looped pipeline system; the expressions of known coefficients C, R, S, T, ϕ are given in the appendix. Therefore, there are four possible leak-induced patterns in the system of Fig. 1(c) for analyzing the leak information by using Eq. (8). Again, these leak-induced patterns are only dependent on the leak information for the specified looped pipeline system. The detailed principle and procedure of applying Eq. (7) and Eq. (8) for leak detection are stated in the following section.

TFR-BASED LEAK DETECTION

It is known from Eq. (7) or Eq. (8) that the leak-induced pattern is dependent of the potential leaking pipe location (pipe number) in the branched or looped pipeline system, which is different from the result of single or simple series pipeline system. Therefore, a traversal calculation and comparison of all the possible leak-induced patterns and leak detection processes is required for such complex pipe systems to find out the most likely or optimal results of the pipe leakage information in the system. For the simple branched and looped pipeline systems focused in this study (e.g., the total number of pipes is less than 6), an enumeration method is used for such calculation and comparison. To obtain accurate and globally optimal result for each leak-induced pattern analysis, the GA-based optimization procedure developed in Duan *et al.* (2012) is used here for the inverse analysis of Eq. (7) or Eq. (8). The detailed formulation and steps for applying this GA-based method in water pipeline systems refer to Duan *et al.* (2012). Figure 3 shows the main application principle and procedure of the proposed TFR-based leak detection method in this study.

It is also noted that, in this proposed method and procedure, the potential leakage information is identified through the fitness comparison of different leak-induced patterns in the given pipeline system. Therefore, as in other transient-based method for pipe defects detection (e.g., Duan *et al.* 2011, 2013, 2014; Lee *et al.* 2013, 2015), the applicability and accuracy of this method may be affected by the model bias/errors (e.g., linear approximation and turbulence) and

system uncertainties (e.g., input and output measurements). The accuracy and limitations of this method are discussed through the applications later in the paper.

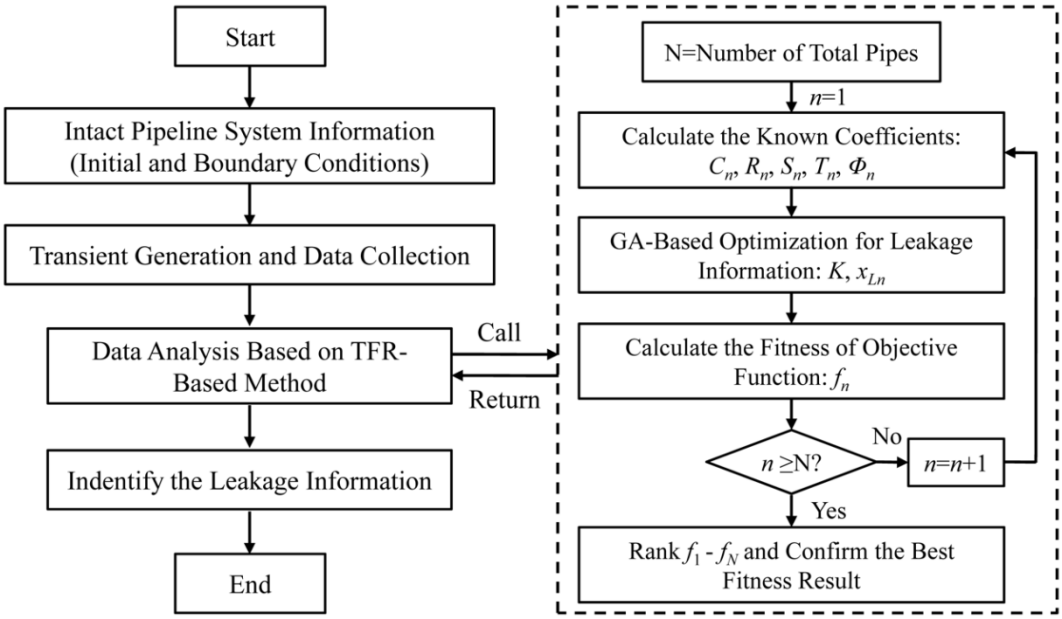

Figure 3: Flowchart of TFR-based leak detection

NUMERICAL VALIDATIONS AND RESULTS ANALYSIS

The system configurations in Figs. 1(b) and 1(c) are firstly used for numerical validations of the proposed TFR-based leak detection method, with the system parameter settings and information given in Table 1. Different leakage cases (location and size) are considered for each test system and shown in Table 2, with tests no. 1 to no. 3 for the branched system and tests no. 4 to no. 7 for the looped system. The system transient responses are obtained by the 1D numerical simulations in the time domain (i.e., Eqs. (1) and (2)). The transient pressure head at the just upstream of the inline valve are collected and then converted by Fourier transform into the frequency domain for the analysis. The results of leakage detection based on the proposed method and procedure in this study are obtained and listed in Table 2. The accuracy of the method is evaluated by the difference between the real and predicted values of the leakage information, which is defined as the relative error (ε) by:

$$\varepsilon(\%) = \frac{\text{predicted value - real value}}{\text{real value}} \times 100 . \tag{9}$$

Based on Eq. (9), the prediction errors for the planned cases are also presented in Table 2. The results demonstrate the validity and accuracy of the proposed method for the leak detection (location and size) in the simple branched and looped pipeline systems. Specifically, the maximum relative errors of the prediction are 13% and 28% respectively for the leakage location and size. That is, this proposed method is more accurate to locate the pipe leakage than to size the leakage, which is similar as the results applied for single and series pipeline systems (Lee *et al.* 2006; Duan *et al.* 2011). This is mainly because of the errors due to the linear approximations in the derivations, which is discussed later in this study.

Table 1: Settings and information of test pipeline systems

System	Pipe length (m)	Pipe size (mm)	Wave speed (m/s)	Pipe friction
no.2 (branched)	l_1 = 500, l_2 = 240; l_3 = 200	D_1 = 500, D_2 = 300; D_3 = 60	a_1 = 1000, a_2 = 1100; a_3 = 1200	$f_1 = f_2 = f_3$ = 0.01
no.3 (looped)	l_1 = 500, l_2 = 300; l_3 = 200; l_4 = 350	D_1 = 500, D_2 = 400; D_3 = 500; D_4 = 200	a_1 = 1000, a_2 = 1100; a_3 = 1000; a_4 = 1200	$f_1 = f_2 = f_3 = f_4$ = 0.01

Table 2: Leakage detection results for branched and looped systems

System	Test no.	Real leakage information		Results of leakage detection			
		x_{Ln} (m)	K_L (10^{-4} m^2/s)	x_{Ln}^P (m)	ε (%)	K_L^P (10^{-4} m^2/s)	ε (%)
Branched pipeline system	1	150 (n=1)	1.0	146	-2.7	0.83	-17
	2	100 (n=2)	3.0	101	1.0	2.84	-5.3
	3	160 (n=3)	2.0	167	4.4	1.85	-7.5
Looped pipeline system	4	300 (n=1)	3.0	281	-6.3	2.68	-10.7
	5	120 (n=2)	1.0	124	3.3	0.97	-3
	6	150 (n=3)	4.0	169	12.7	3.69	-7.8
	7	100 (n=4)	0.8	113	13	0.58	27.5

To further demonstrate the detection process and results, the leak-induced patterns of tests no. 1 and no. 4 from the numerical simulations by 1D models and theoretical prediction by Eq. (7) or (8) are plotted in Fig. 4 for comparison. Both the results in Table 2 and Fig. 4 indicate the good agreements of the phase changes between the leak-induced patterns by numerical simulations and analytical analysis, which results in the relatively small errors in the prediction of the leak locations in Table 2. However, the results also reveal overall that the analytical result of Eq. (7) or (8) has underestimated the amplitudes of the leak-induced patterns due to the simplifications of the nonlinear effects of friction term during the derivations, which also results in the relatively

large and negative errors of the leak size prediction in Table 2. In this regard, the inclusion of nonlinearities of transient effects in the system (e.g., friction or turbulence or wave-structure interactions) is required to improve the accuracy of the leak detection results for the proposed method. This aspect may become the next-step work in the future for the improvement of the TFR-based defect detection method.

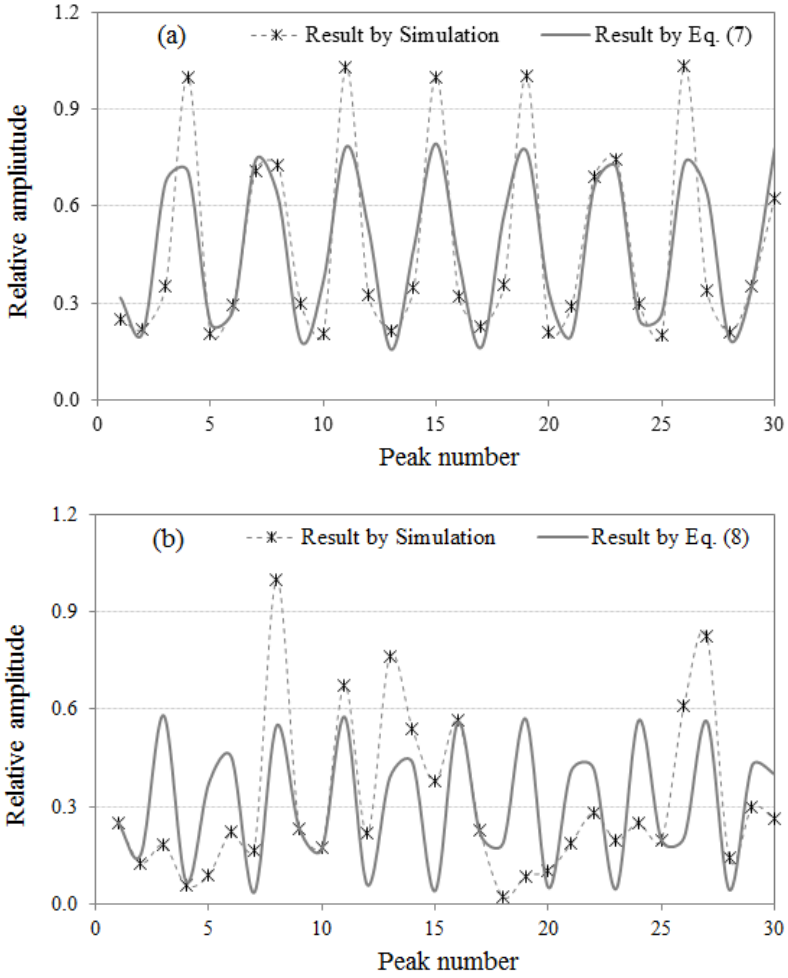

Figure 4: Leak-induced patterns of system TFR results: (a) test no. 1; (b) test no. 4

FURTHER APPLICATION AND DISCUSSION

The application results and analysis above have validated and confirmed the applicability and accuracy of the proposed method and application procedure for pipe leak detection in the simple branched and looped pipeline systems considered in this study. These successful validations

provide the possibility of the extension of the TFR-based method for leak detection to complex pipe networks consisting of multiple branched and looped junctions. From this perspective, and based on the similar procedures of this study, the TRF results for multiple junctions (branched and looped) can also be derived for such more complex pipe systems, which actually results a similar form of leak-induced patterns given in this study, but with different expressions of the known-system based coefficients (e.g., C, R, S, T, and ϕ). The details are neglected in this study for the space limitation, but a complex system with two branched junctions shown in Fig. 5 is adopted for this exploration. The information of system configurations and parameters are plotted in Fig. 5, with different leakage test cases (no. 8 to no. 12) listed in Table 3.

Table 3: Leakage detection results for the system with two branched pipe junctions

Test no.	Real leakage information		Results of leakage detection			
	x_{Ln} (m)	K_L (10^{-4} m^2/s)	x_{Ln}^P (m)	ε (%)	K_L^P (10^{-4} m^2/s)	ε (%)
8	300 (n=1)	2.0	346	15.3	1.36	-32.0
9	150 (n=2)	1.2	141	-6.0	0.78	-35.0
10	210 (n=3)	0.5	216	2.9	0.43	-14.0
11	140 (n=4)	5.0	157	12.1	4.65	-7.0
12	80 (n=5)	3.0	84	5.0	2.49	-17.0

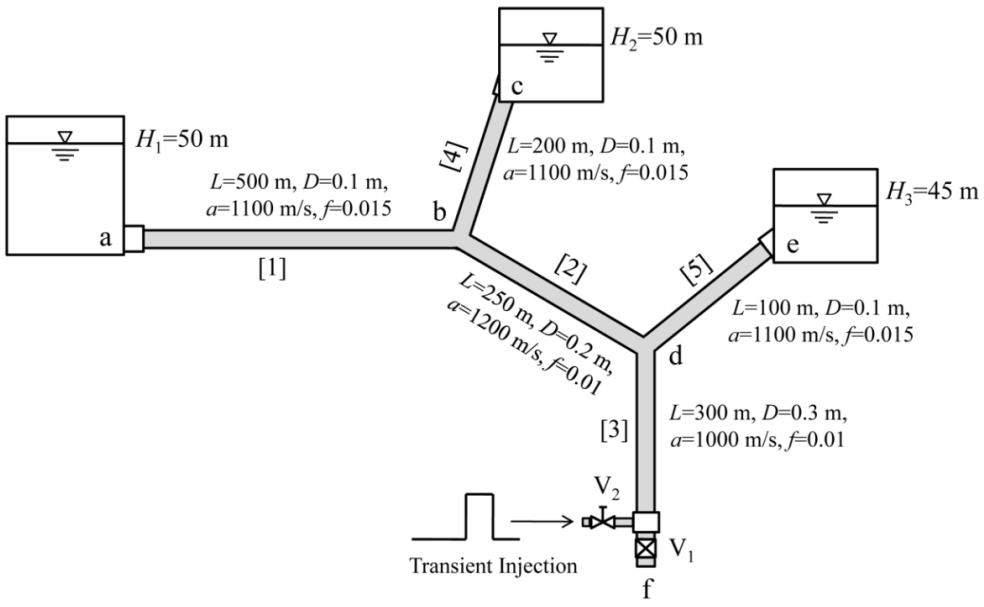

Figure 5: Test pipeline system with two branched junctions

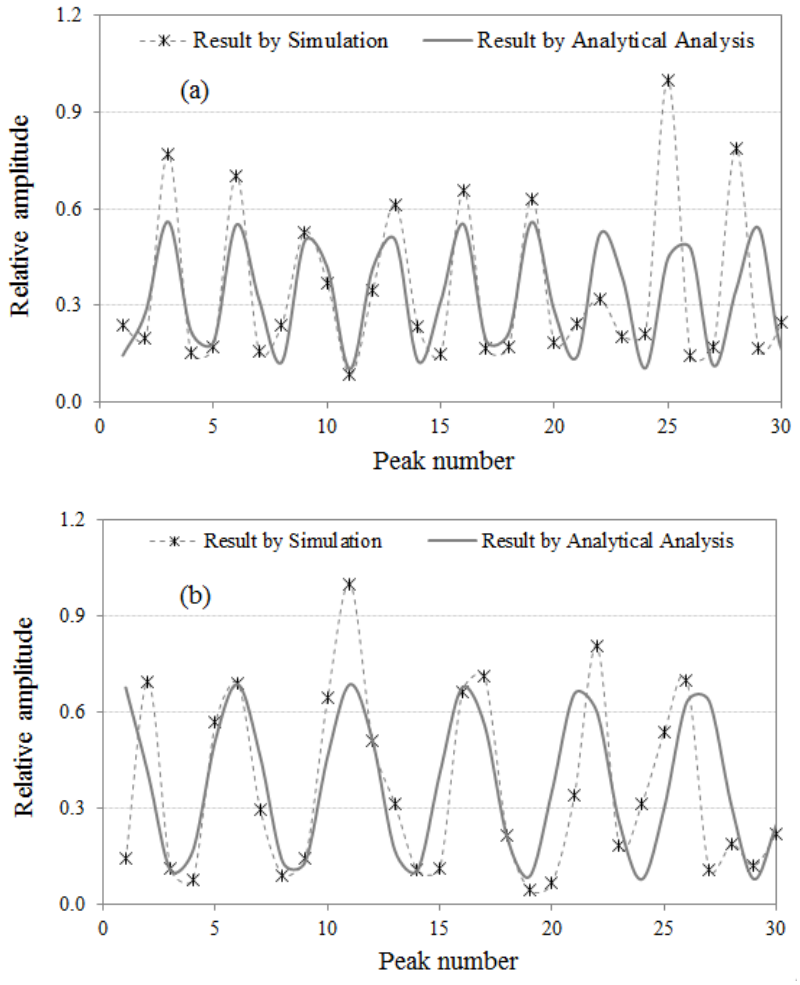

Figure 6: Leak-induced patterns of system TFR results: (a) test no. 8; (b) test no. 10

The TRF-based leak detection results by the method and procedure proposed in this study are shown in Table 3 and the obtained leak-induced patterns for tests no. 8 and no. 10 are plotted in Fig. 6, which demonstrate again the applicability of the TRF-based method for identifying and detecting pipe leakage in complex pipe systems. Compared to the simple branched pipe system in Fig. 1(b), the detection accuracy of the TFR-based method becomes decreased with the increase of the connection complexities of the system. However, the relative errors are still within 16% and 35% for leakage location and size respectively, which may provide useful information and significant implications for the pipe leakage detection and diagnosis of practical water supply pipe systems. From this point of view, the TFR-based leak detection method is extendable and applicable to complex pipeline networks, as long as the pipe system under

investigation has been pre-defined for the topological configurations and the system properties and operation parameters are well known for the analysts under the original and intact conditions (before the occurrence of leakage).

While the successful applications of the developed TFR-based method for leakage detection in complex pipeline systems with single and multiple branched junctions and simple looped junction respectively, the application results also reveal the obvious increase of the detection errors with system complexities (e.g., number of junctions), especially for predicting the leakage size. This result and trend may be attributed to following factors:

(1) inaccuracies of the TFR method from the analytical derivations: which mainly include the linearization of steady friction term; neglect of frequency dependent friction effect; assumption of relatively small leakage capacity to main pipeline discharge;

(2) errors of data collections from the numerical simulations (or measurement in practical applications): such as sample frequency of the time-domain data; trace cutting length of time-domain data (e.g., number of periods for data analysis); and the discrete Fourier transform for frequency data analysis; and

(3) uncertainties of the inverse analysis (e.g., GA-based optimization in this study): the convergence and error of inverse analysis process; and the non-uniqueness of solutions to the leak-induced patterns for complex pipe systems.

With these limitations and influence factors, it is necessary to improve the transient model and methods for the accurate extension and application of the developed TFR-based leak detection in practical and complex pipe systems, for example, through following aspects:

(a) improvement of 1D transient models (in time and frequency domains) to accurately represent the physics and process of transient pipe flows in complex pipe systems such as unsteady friction and turbulence, wave-junction interaction, and wave-leak interaction;

(b) selection of the best injected transient signals to capture the full picture of the leakage characteristics, for example appropriate bandwidth of signals as suggested in Duan *et al.* (2010, 2011);

(c) algorithm of the inverse analysis for obtaining globally optimal and physical solutions of the leak-induced patterns, especially for large-scale and complex pipe networks.

Finally, it is important to point out that only the numerical applications are conducted in this paper for the preliminary validations of the developed TFR-based leak detection method. In the

future work, further experimental tests (laboratory and field) are required and designed to validate and verify the accuracy, tolerance and sensitivity of this developed method for practical cases under the influences of inevitable noises and uncertainties in the system.

SUMMARY AND CONCLUSIONS

This paper investigates the possibility of the application of the TFR-based leak detection method in complex pipeline systems. The systems of simple branched and looped pipeline junctions are considered and investigated in this study. The influence of different pipe junctions to system transient responses is firstly examined by numerical simulations in the time and frequency domains, which highlights the merits of the frequency domain responses for characterizing the transient system behaviors. On this point, the system TFRs are derived by the transfer matrix method for both the branched and looped pipe systems, which are then used for the detection of pipe leakage information in this study.

The analytical results indicate that both the branched and looped pipe systems may have great influences to the system TFRs but have little impacts on the leak-induced patterns. The GA-based optimization is then proposed for solving the analytical leak-induced patterns to obtain the leakage information in the system. The developed TFR-based method and application procedure are validated through different numerical tests for pipe systems with single branched, single looped and two branched pipe junctions respectively. The results demonstrate the applicability and accuracy of the developed method for leakage identification and detection in complex pipe systems. However, the applications also imply that this method is more accurate to locate the pipe leakage than to size the leakage in complex pipeline systems.

The results analysis and discussion of this study provide the evidences and confirmations for the extension of the TFR-based method to complex pipe networks. It is also noted that extensive experimental tests are demanded in the future work for further validating the accuracy and sensitivity of the proposed method in practical water pipeline systems with different connection complexities.

ACKNOWLEDGEMENTS

This paper was partially supported by the research grants from the Hong Kong Polytechnic University (HKPU) under projects with numbers 1-ZVCD, 1-ZVGF, G-YBC9 and G-YBHR.

The author would like to thank Mr Tony Che for his kind help on preparing and plotting the figures in this paper.

APPENDIX – DERIVATIONS OF THE TFR RESULTS

(A) For branched pipeline system:

The transfer matrix at the branched junction has a following form (Chaudhry 1987),

$$P=\begin{bmatrix}1 & Z\\ 0 & 1\end{bmatrix}, \tag{A1}$$

in which Z represent the discharge impendence factor due to the branched pipeline. For example, when the boundary of the pipe branch is constant-head reservoir as shown in Fig. 1(b), it has,

$$Z=\frac{U_{22}^{br}}{U_{21}^{br}}, \tag{A2}$$

in which U_{ij}^{br} is the element of the lumped transfer matrix for the branched pipeline (which can be single or series pipeline). Therefore, the TFR of the intact (leak-free) branched pipe system in Fig. 1(b) can be obtained by transfer matrix multiplication principle as (Duan & Lee 2015),

$$\begin{Bmatrix}q\\ h\end{Bmatrix}^{b}=\begin{bmatrix}\cos(\mu_2 l_2) & i\frac{1}{Y_2}\sin(\mu_2 l_2)\\ iY_2\sin(\mu_2 l_2) & \cos(\mu_2 l_2)\end{bmatrix}\begin{bmatrix}1 & Z_{c3}\\ 0 & 1\end{bmatrix}\begin{bmatrix}\cos(\mu_1 l_1) & i\frac{1}{Y_1}\sin(\mu_1 l_1)\\ iY_1\sin(\mu_1 l_1) & \cos(\mu_1 l_1)\end{bmatrix}\begin{Bmatrix}q\\ h\end{Bmatrix}^{a}, \tag{A3}$$

or,

$$\begin{Bmatrix}q\\ h\end{Bmatrix}^{b}=\begin{bmatrix}\cos(\mu_2 l_2) & i\frac{1}{Y_2}\sin(\mu_2 l_2)\\ iY_2\sin(\mu_2 l_2) & \cos(\mu_2 l_2)\end{bmatrix}\begin{bmatrix}1 & Z_{c1}\\ 0 & 1\end{bmatrix}\begin{bmatrix}\cos(\mu_3 l_3) & i\frac{1}{Y_3}\sin(\mu_3 l_3)\\ iY_3\sin(\mu_3 l_3) & \cos(\mu_3 l_3)\end{bmatrix}\begin{Bmatrix}q\\ h\end{Bmatrix}^{d}, \tag{A4}$$

along the two possible pipe flow directions of *a*-*c*-*b* and *d*-*c*-*b* respectively. That is, in this two flow directions, the pipe 3 and pipe 1 are treated as branched section respectively (Duan & Lee 2015). As a result, the transient pressure heads at downstream end *b* for the above two cases can be obtained respectively as,

$$h^b=-\frac{iY_2\sin(\mu_2 l_2)\cos(\mu_1 l_1)-Z_{C3}Y_2Y_1\sin(\mu_2 l_2)\sin(\mu_1 l_1)+iY_1\cos(\mu_2 l_2)\sin(\mu_1 l_1)}{\cos(\mu_2 l_2)\cos(\mu_1 l_1)-\frac{Y_1}{Y_2}\sin(\mu_2 l_2)\sin(\mu_1 l_1)+iY_1Z_{C3}\cos(\mu_2 l_2)\sin(\mu_1 l_1)}, \tag{A5}$$

$$h^b=-\frac{iY_2\sin(\mu_2 l_2)\cos(\mu_3 l_3)-Z_{C1}Y_2Y_3\sin(\mu_2 l_2)\sin(\mu_3 l_3)+iY_3\cos(\mu_2 l_2)\sin(\mu_3 l_3)}{\cos(\mu_2 l_2)\cos(\mu_3 l_3)-\frac{Y_3}{Y_2}\sin(\mu_2 l_2)\sin(\mu_3 l_3)+iY_3Z_{C1}\cos(\mu_2 l_2)\sin(\mu_3 l_3)}, \tag{A6}$$

Therefore, the singularity (resonance) conditions are given by,

$$\cos(\mu_2 l_2)\cos(\mu_1 l_1)-\frac{Y_1}{Y_2}\sin(\mu_2 l_2)\sin(\mu_1 l_1)+iY_1 Z_{C3}\cos(\mu_2 l_2)\sin(\mu_1 l_1)=0, \tag{A7}$$

$$\cos(\mu_2 l_2)\cos(\mu_3 l_3)-\frac{Y_3}{Y_2}\sin(\mu_2 l_2)\sin(\mu_3 l_3)+iY_3 Z_{C1}\cos(\mu_2 l_2)\sin(\mu_3 l_3)=0. \tag{A8}$$

According to Duan & Lee (2015),

$$Z_{c3}=\frac{\cos(\mu_3 l_3)}{iY_3\sin(\mu_3 l_3)};\ Z_{c1}=\frac{\cos(\mu_1 l_1)}{iY_1\sin(\mu_1 l_1)}, \tag{A9}$$

which gives the identical result for both cases as,

$$\begin{bmatrix} Y_3Y_2\sin(\mu_3 l_3)\cos(\mu_2 l_2)\cos(\mu_1 l_1) \\ -Y_3Y_1\sin(\mu_3 l_3)\sin(\mu_2 l_2)\sin(\mu_1 l_1) \\ +Y_2Y_1\cos(\mu_3 l_3)\cos(\mu_2 l_2)\sin(\mu_1 l_1) \end{bmatrix}=0. \tag{A10}$$

That is, the resonant condition for this branched system is unique, no matter which flow path is considered for the analysis.

Under pipe leakage situation, three possible cases where the single leak is located at each of the three pipe sections respectively are existed in this system, which are considered individually as below:

(1) Leak is located on pipe 1, gives

$$\begin{Bmatrix} q \\ h \end{Bmatrix}^b=\begin{bmatrix} \cos(\mu_2 l_2) & i\frac{1}{Y_2}\sin(\mu_2 l_2) \\ iY_2\sin(\mu_2 l_2) & \cos(\mu_2 l_2) \end{bmatrix}\begin{bmatrix} 1 & Z_{C3} \\ 0 & 1 \end{bmatrix}$$
$$\begin{bmatrix} \cos(\mu_1 x_2) & i\frac{1}{Y_1}\sin(\mu_1 x_2) \\ iY_1\sin(\mu_1 x_2) & \cos(\mu_1 x_2) \end{bmatrix}\begin{bmatrix} 1 & -K \\ 0 & 1 \end{bmatrix}\begin{bmatrix} \cos(\mu_1 x_1) & i\frac{1}{Y_1}\sin(\mu_1 x_1) \\ iY_1\sin(\mu_1 x_1) & \cos(\mu_1 x_1) \end{bmatrix}\begin{Bmatrix} q \\ h \end{Bmatrix}^a, \tag{A11}$$

(2) Leak is located on pipe 3, gives

$$\begin{Bmatrix} q \\ h \end{Bmatrix}^b=\begin{bmatrix} \cos(\mu_2 l_2) & i\frac{1}{Y_2}\sin(\mu_2 l_2) \\ iY_2\sin(\mu_2 l_2) & \cos(\mu_2 l_2) \end{bmatrix}\begin{bmatrix} 1 & Z_{C1} \\ 0 & 1 \end{bmatrix}$$
$$\begin{bmatrix} \cos(\mu_3 y_2) & i\frac{1}{Y_3}\sin(\mu_3 y_2) \\ iY_3\sin(\mu_3 y_2) & \cos(\mu_3 y_2) \end{bmatrix}\begin{bmatrix} 1 & -K \\ 0 & 1 \end{bmatrix}\begin{bmatrix} \cos(\mu_3 y_1) & i\frac{1}{Y_3}\sin(\mu_3 y_1) \\ iY_3\sin(\mu_3 y_1) & \cos(\mu_3 y_1) \end{bmatrix}\begin{Bmatrix} q \\ h \end{Bmatrix}^a, \tag{A12}$$

(3) Leak is located on pipe 2, gives

$$\begin{Bmatrix} q \\ h \end{Bmatrix}^b = \begin{bmatrix} \cos(\mu_2 z_2) & i\frac{1}{Y_2}\sin(\mu_2 z_2) \\ iY_2\sin(\mu_2 z_2) & \cos(\mu_2 z_2) \end{bmatrix} \begin{bmatrix} 1 & -K \\ 0 & 1 \end{bmatrix} \begin{bmatrix} \cos(\mu_2 z_1) & i\frac{1}{Y_2}\sin(\mu_2 z_1) \\ iY_2\sin(\mu_2 z_1) & \cos(\mu_2 z_1) \end{bmatrix} \begin{bmatrix} 1 & Z_{C3} \\ 0 & 1 \end{bmatrix} \begin{bmatrix} \cos(\mu_1 l_1) & i\frac{1}{Y_1}\sin(\mu_1 l_1) \\ iY_1\sin(\mu_1 l_1) & \cos(\mu_1 l_1) \end{bmatrix} \begin{Bmatrix} q \\ h \end{Bmatrix}^a, \tag{A13}$$

in which $x_1+x_2=l_1$; $y_1+y_2=l_3$; $z_1+z_2=l_2$; K_L = the impendence factor of the leak orifice and $K_L = Q_{L0}/2H_{L0}$ with Q_{L0} and H_{L0} are steady state discharge and head difference at the leak orifice in the given system (Duan *et al.* 2011). Correspondingly, after the mathematical manipulations and essential simplifications (Lee *et al.* 2006; Duan *et al.* 2011; Duan & Lee 2015), the TFR results at the downstream of the system (e.g., node *b*) are derived as:

$$\frac{1}{h_{L1}^b} = \frac{K_L}{C_1^B}\left[1-\cos\left(2\mu_1 x_1 + \phi_1^B\right)\right], \tag{A14}$$

$$\frac{1}{h_{L2}^b} = \frac{K_L}{C_2^B}\left[1-\cos\left(2\mu_3 y_1 + \phi_2^B\right)\right], \tag{A15}$$

$$\frac{1}{h_{L3}^b} = \frac{K_L}{C_3^B}\left[1-\cos\left(2\mu_2 z_2 + \phi_3^B\right)\right], \tag{A16}$$

where C_1^B, C_2^B, C_3^B and ϕ_1^B, ϕ_2^B, ϕ_3^B are intact system based known coefficients for specific frequencies, and, for the considered branched system in Fig. 1(b), $\phi_1^B = \phi_2^B = 0$; $\phi_3^B = \pi/2$;

$$C_1^B = \frac{2\sin(\mu_1 l_1)}{\cos(\mu_2 l_2)}\left[\cos(\mu_2 l_2)\sin(\mu_1 l_1) + \frac{Y_2}{Y_1}\sin(\mu_2 l_2)\cos(\mu_1 l_1) + \frac{Y_2}{Y_3}\frac{\cos(\mu_3 l_3)\sin(\mu_2 l_2)\sin(\mu_1 l_1)}{\sin(\mu_3 l_3)}\right]; \tag{A17}$$

$$C_2^B = \frac{2\sin(\mu_3 l_3)}{\cos(\mu_2 l_2)}\left[\cos(\mu_2 l_2)\sin(\mu_3 l_3) + \frac{Y_2}{Y_3}\sin(\mu_2 l_2)\cos(\mu_3 l_3) + \frac{Y_2}{Y_1}\frac{\sin(\mu_3 l_3)\sin(\mu_2 l_2)\cos(\mu_1 l_1)}{\sin(\mu_1 l_1)}\right]; \tag{A18}$$

$$C_3^B = \frac{2\cos(\mu_2 l_2)}{\sin(\mu_1 l_1)}\left[\frac{Y_2}{Y_1}\sin(\mu_2 l_2)\cos(\mu_1 l_1) + \cos(\mu_2 l_2)\sin(\mu_1 l_1) + \frac{Y_2}{Y_3}\frac{\cos(\mu_3 l_3)\sin(\mu_1 l_1)\sin(\mu_2 l_2)}{\sin(\mu_3 l_3)}\right]. \tag{A19}$$

Consequently, a general form of the TFR results can be summarized for the branched pipeline system in Fig. 1(b) as expressed in Eq. (7) in the text.

(B) For looped pipeline system:

For the looped system in Fig. 1(c), there are two branch junctions in the system, but without any explicit boundary for describing the branches (e.g., constant-head reservoir or dead-end as for the branched system in Fig. 1(b)). In this study, the loop is considered as a "loop point" consisting of two parallel pipes, so that its equivalent transfer matrix can be derived and applied appropriately. Based on the results of single or series pipe section in Eq. (3), the transfer matrix equations for the branched pipes 3 & 4, respectively, are

$$\begin{Bmatrix} \hat{q} \\ \hat{h} \end{Bmatrix}_3^R = \begin{bmatrix} v_{11} & v_{12} \\ v_{21} & v_{22} \end{bmatrix} \begin{Bmatrix} \hat{q} \\ \hat{h} \end{Bmatrix}_3^L ; \quad \begin{Bmatrix} \hat{q} \\ \hat{h} \end{Bmatrix}_4^R = \begin{bmatrix} u_{11} & u_{12} \\ u_{21} & u_{22} \end{bmatrix} \begin{Bmatrix} \hat{q} \\ \hat{h} \end{Bmatrix}_4^L , \tag{B1}$$

where the transfer matrix elements *v*, *u* are known based on the intact system configurations as shown in Eq. (3). Meanwhile, considering the continuity and energy conservation relationships at the both branched junctions *c* and *d*, it has (ignoring minor loss here),

$$\begin{matrix} q_1^R = \hat{q}_3^L + \hat{q}_4^L \\ h_1^R = \hat{h}_3^L = \hat{h}_4^L \end{matrix} ; \quad \begin{matrix} q_2^L = \hat{q}_3^R + \hat{q}_4^R \\ h_2^L = \hat{h}_3^R = \hat{h}_4^R \end{matrix} . \tag{B2}$$

Combining Eq. (B1) and Eq. (B2) provides,

$$\begin{matrix} q_2^L = \alpha q_1^R + \beta h_1^R \\ h_2^L = \phi q_1^R + \gamma h_1^R \end{matrix} , \tag{B3}$$

where $\alpha, \beta, \phi, \gamma$ are known coefficients for the given intact system, and

$$\alpha = \frac{v_{11}u_{21} + v_{21}u_{11}}{v_{21} + u_{21}} ; \ \beta = \frac{(v_{12} + u_{12})(v_{21} + u_{21}) - (u_{11} - v_{11})(u_{22} - v_{22})}{v_{21} + u_{21}} ;$$

$$\phi = \frac{u_{21}v_{21}}{v_{21} + u_{21}} ; \ \gamma = \frac{u_{22}v_{21} + u_{21}v_{22}}{v_{21} + u_{21}} .$$

That is, for the "loop point", it has the form,

$$\begin{Bmatrix} q \\ h \end{Bmatrix}_{Loop}^{RHS} = \begin{bmatrix} \alpha & \beta \\ \phi & \gamma \end{bmatrix} \begin{Bmatrix} q \\ h \end{Bmatrix}_{Loop}^{LHS} , \tag{B4}$$

where superscripts *LHS* and *RHS* denote the quantities for the left hand side and right hand side of the "loop point". As a result, the transfer matrix equation for the intact looped pipe system of Fig. 1(c) can be described by,

$$\begin{Bmatrix} q \\ h \end{Bmatrix}^b = \begin{bmatrix} \cos(\mu_2 l_2) & i\frac{1}{Y_2}\sin(\mu_2 l_2) \\ iY_2\sin(\mu_2 l_2) & \cos(\mu_2 l_2) \end{bmatrix} \begin{bmatrix} \alpha & \beta \\ \phi & \gamma \end{bmatrix} \begin{bmatrix} \cos(\mu_1 l_1) & i\frac{1}{Y_1}\sin(\mu_1 l_1) \\ iY_1\sin(\mu_1 l_1) & \cos(\mu_1 l_1) \end{bmatrix} \begin{Bmatrix} q \\ h \end{Bmatrix}^a = \begin{bmatrix} U_{11} & U_{12} \\ U_{21} & U_{22} \end{bmatrix} \begin{Bmatrix} q \\ h \end{Bmatrix}^a, \tag{B5}$$

where U is the lumped transfer matrix element. With applying similar operations in the previous studies for series and branched pipeline systems (Duan *et al.* 2011; Duan & Lee 2015), the resonant conditions for this looped system is governed by,

$$\left[\alpha\cos(\mu_2 l_2)\cos(\mu_1 l_1) - \frac{\gamma Y_1}{Y_2}\sin(\mu_2 l_2)\sin(\mu_1 l_1)\right] + i\left[\beta Y_1\cos(\mu_2 l_2)\sin(\mu_1 l_1) + \frac{\phi}{Y_2}\sin(\mu_2 l_2)\cos(\mu_1 l_1)\right] = 0. \tag{B6}$$

Under pipe leakage condition for the considered system in Fig. 1(c), four possible leakage cases are existed: the leakage is located on pipes 1, 2, 3, 4 respectively. For illustration, the derivations of the cases for the leakage on pipe 1 and 3 are provided below, and the other two cases can be achieved with similar procedures.

(1) Leakage is on pipe 1 (or on pipe 2 using similar analysis):

$$\begin{Bmatrix} q \\ h \end{Bmatrix}^b = \begin{bmatrix} \cos(\mu_2 l_2) & i\frac{1}{Y_2}\sin(\mu_2 l_2) \\ iY_2\sin(\mu_2 l_2) & \cos(\mu_2 l_2) \end{bmatrix} \begin{bmatrix} \alpha & \beta \\ \phi & \gamma \end{bmatrix} \begin{bmatrix} \cos(\mu_1 x_2) & i\frac{1}{Y_1}\sin(\mu_1 x_2) \\ iY_1\sin(\mu_1 x_2) & \cos(\mu_1 x_2) \end{bmatrix} \begin{bmatrix} 1 & -K \\ 0 & 1 \end{bmatrix} \begin{bmatrix} \cos(\mu_1 x_1) & i\frac{1}{Y_1}\sin(\mu_1 x_1) \\ iY_1\sin(\mu_1 x_1) & \cos(\mu_1 x_1) \end{bmatrix} \begin{Bmatrix} q \\ h \end{Bmatrix}^a, \tag{B7}$$

where $x_1 + x_2 = l_1$;

(2) Leak is within the loop *c-d* and on pipe 3 (or on pipe 4 using similar analysis):

$$\begin{Bmatrix} q \\ h \end{Bmatrix}^b = \begin{bmatrix} \cos(\mu_2 l_2) & i\frac{1}{Y_2}\sin(\mu_2 l_2) \\ iY_2\sin(\mu_2 l_2) & \cos(\mu_2 l_2) \end{bmatrix} \begin{bmatrix} \alpha^L & \beta^L \\ \phi^L & \gamma^L \end{bmatrix} \begin{bmatrix} \cos(\mu_1 l_1) & i\frac{1}{Y_1}\sin(\mu_1 l_1) \\ iY_1\sin(\mu_1 l_1) & \cos(\mu_1 l_1) \end{bmatrix} \begin{Bmatrix} q \\ h \end{Bmatrix}^a, \tag{B8}$$

with:

$$\begin{Bmatrix} \hat{q} \\ \hat{h} \end{Bmatrix}_3^{RHS} = \begin{bmatrix} \cos(\mu_3 z_2) & i\frac{1}{Y_3}\sin(\mu_3 z_2) \\ iY_3\sin(\mu_3 z_2) & \cos(\mu_3 z_2) \end{bmatrix} \begin{bmatrix} 1 & -K \\ 0 & 1 \end{bmatrix} \begin{bmatrix} \cos(\mu_3 z_1) & i\frac{1}{Y_3}\sin(\mu_3 z_1) \\ iY_3\sin(\mu_3 z_1) & \cos(\mu_3 z_1) \end{bmatrix} \begin{Bmatrix} \hat{q} \\ \hat{h} \end{Bmatrix}_3^{LHS}, \tag{B9}$$

and

$$\begin{Bmatrix} q \\ h \end{Bmatrix}_{Loop-L}^{RHS} = \begin{bmatrix} \alpha^L & \beta^L \\ \phi^L & \gamma^L \end{bmatrix} \begin{Bmatrix} q \\ h \end{Bmatrix}_{Loop-L}^{LHS}, \tag{B10}$$

where $z_1+z_2=l_3$; subscript *Loop-L* represents the quantities for the "loop point" under leakage condition.

After mathematical manipulations and re-arrangements, the final TFR results for these two cases at the downstream are obtained as,

$$\frac{1}{h_{L1}^b} = \frac{1}{C_1^O}\left[R_1^O + \sqrt{\left(S_1^O\right)^2 + \left(T_1^O\right)^2}\,\sin\left(\mu_1 l_1 - 2\mu_1 x_2 + \phi_1^O\right)\right], \tag{B11}$$

$$\frac{1}{h_{L3}^b} = \frac{1}{C_3^O}\left[R_3^O + \sqrt{\left(S_3^O\right)^2 + \left(T_3^O\right)^2}\,\sin\left(\mu_3 l_3 - 2\mu_3 z_2 + \phi_3^O\right)\right], \tag{B12}$$

where: $C_1{}^O$, $C_3{}^O$, $R_1{}^O$, $R_3{}^O$, $S_1{}^O$, $S_3{}^O$, $T_1{}^O$, $T_3{}^O$, $\phi_1{}^O$, $\phi_3{}^O$, are intact pipe system based known coefficients, and

$$C_1^O = -\frac{2F_1}{Y_1};\ C_3^O = -\frac{2F_3}{Y_3};\ \phi_1^O = \arctan\left(\frac{S_1^O}{T_1^O}\right);\ \phi_3^O = \arctan\left(\frac{S_3^O}{T_3^O}\right);$$

$$F_1 = F_3 = \begin{bmatrix} \alpha Y_2 \sin(\mu_2 l_2)\cos(\mu_1 l_1) + \gamma Y_1 \cos(\mu_2 l_2)\sin(\mu_1 l_1) \\ -i\phi\cos(\mu_2 l_2)\cos(\mu_1 l_1) + i\beta Y_2 Y_1 \sin(\mu_2 l_2)\sin(\mu_1 l_1) \end{bmatrix};$$

$$R_1^O = \begin{bmatrix} -\gamma\cos(\mu_2 l_2)\sin(\mu_1 l_1) - \alpha\dfrac{Y_1}{Y_2}\sin(\mu_2 l_2)\cos(\mu_1 l_1) \\ -i\dfrac{\phi}{Y_2}\sin(\mu_2 l_2)\sin(\mu_1 l_1) + i\beta Y_1\cos(\mu_2 l_2)\cos(\mu_1 l_1) \end{bmatrix};$$

$$R_3^O = \begin{bmatrix} -Y_3\cos(\mu_4 l_4)\cos(\mu_3 l_3)\cos(\mu_2 l_2)\cos(\mu_1 l_1) + \dfrac{Y_3 Y_1}{Y_4}\sin(\mu_4 l_4)\cos(\mu_3 l_3)\cos(\mu_2 l_2)\sin(\mu_1 l_1) \\ +\dfrac{Y_4 Y_3}{Y_2}\sin(\mu_4 l_4)\cos(\mu_3 l_3)\sin(\mu_2 l_2)\cos(\mu_1 l_1) + \dfrac{Y_3 Y_1}{Y_2}\cos(\mu_4 l_4)\cos(\mu_3 l_3)\sin(\mu_2 l_2)\sin(\mu_1 l_1) \\ +Y_4\sin(\mu_4 l_4)\sin(\mu_3 l_3)\cos(\mu_2 l_2)\cos(\mu_1 l_1) - \dfrac{Y_4 Y_1}{Y_2}\sin(\mu_4 l_4)\sin(\mu_3 l_3)\sin(\mu_2 l_2)\sin(\mu_1 l_1) \\ +\dfrac{Y_4 Y_1}{Y_3}\sin(\mu_4 l_4)\cos(\mu_3 l_3)\cos(\mu_2 l_2)\sin(\mu_1 l_1) + 2Y_1\cos(\mu_4 l_4)\sin(\mu_3 l_3)\cos(\mu_2 l_2)\sin(\mu_1 l_1) \end{bmatrix};$$

$$S_1^O = \left[\alpha\frac{Y_1}{Y_2}\sin(\mu_2 l_2) - i\beta Y_1\cos(\mu_2 l_2)\right];$$

$$S_3^O = \begin{bmatrix} Y_3\cos(\mu_4 l_4)\cos(\mu_2 l_2)\cos(\mu_1 l_1) - \dfrac{Y_3 Y_1}{Y_4}\sin(\mu_4 l_4)\cos(\mu_2 l_2)\sin(\mu_1 l_1) \\ -\dfrac{Y_4 Y_3}{Y_2}\sin(\mu_4 l_4)\sin(\mu_2 l_2)\cos(\mu_1 l_1) + \dfrac{Y_4 Y_1}{Y_3}\sin(\mu_4 l_4)\cos(\mu_2 l_2)\sin(\mu_1 l_1) \\ -\dfrac{Y_3 Y_1}{Y_2}\cos(\mu_4 l_4)\sin(\mu_2 l_2)\sin(\mu_1 l_1) \end{bmatrix};$$

$$T_1^O = -\left[\alpha\cos(\mu_2 l_2) + i\frac{\phi}{Y_2}\sin(\mu_2 l_2)\right];$$

$$T_3^O = -\left[\frac{Y_4 Y_1}{Y_2}\sin(\mu_4 l_4)\sin(\mu_2 l_2)\sin(\mu_1 l_1) + Y_4\sin(\mu_4 l_4)\cos(\mu_2 l_2)\cos(\mu_1 l_1)\right].$$

As a result, the TRF results of the looped pipeline system can be expressed with a general form of Eq. (8) in the text.

REFERENCES

Brunone, B. (1999). Transient test-based technique for leak detection in outfall pipes. *J. Water Resources Planning and Management*, ASCE, 125(5), 302-306.

Brunone, B., and Ferrante, M. (2001). Detecting leaks in pressurized pipes by means of transients. *J. Hydraulic Res.* IAHR, 39(4), 1-9.

Brunone, B., Ferrante, M., and Meniconi, S. (2008). Discussion of 'Detection of partial blockage in single pipelines' by Mohapatra, P.K., Chaudhry, M.H., Kassem, A.A., and Moloo, J. *J. of Hydraulic Engineering*, ASCE, 134(6), 872-874.

Chaudhry, M. (1987). *Applied hydraulic transients*. Van Nostrand Reinhold, New York.

Colombo, A.F., Lee, P.J., and Karney, B.W. (2009). A selective literature review of transient-based leak detection methods. *J. Hydro-environment Research*, IAHR, 2(4), 212-227.

Covas, D., Ramos, H., Graham, N., and Maksimovic, C. (2004). Application of hydraulic transients for leak detection in water supply systems. *Water Science and Technology: Water Supply*, IWA, 4(5-6), 365-374.

Covas, D., Ramos, H., Almeida, A.B. (2005). Standing wave difference method for leak detection in pipeline systems. *J. Hydraulic Eng.* ASCE, 131(12), 1106-1116.

Covas, D., and Ramos, H. (2010). Case studies of leak detection and location in water pipe systems by inverse transient analysis. *J. Water Res. Plan. and Manage.*, 136(2), 248-257.

Duan, H.F., Ghidaoui, M.S., Lee, P.J., and Tung, Y.K. (2010). Essential system response information for transient-based leak detection methods. *J. Hydraulic Res.* IAHR, 48(5), 650-657.

Duan, H.F., Lee, P.J., Ghidaoui, M.S., and Tung, Y.K. (2011). Leak detection in complex series pipelines by using system frequency response method. *J. Hydraulic Res.*, IAHR, 49(2), 213-221.

Duan, H.F., Lee, P.J., Ghidaoui, M.S., and Tung, Y.K. (2012). System response function based leak detection in viscoelastic pipeline. *J. Hydraulic Eng.* ASCE, 138(2), 143-153.

Duan, H.F., Lee, P.J., Ghidaoui, M.S., and Tuck J. (2014). Transient wave-blockage Interaction and extended blockage detection in pressurized pipes, *J. Fluids & Structure*, 46(2014), 2-16.

Duan, H.F., and Lee, P.J., (2015). Transient-based frequency domain method for dead-end side branch detection in reservoir-pipeline-valve systems. *J. Hydraulic Eng.* ASCE, DOI: 10.1061/(ASCE) HY.1943-7900.0001070 , 04015042.

Ferrante, M., and Brunone, B. (2003). Pipe system diagnosis and leak detection by unsteady-state tests-1: Harmonic analysis. *Advances in Water Res.* 26(1), 95-105.

Lee, P.J. (2005). Using system response functions of liquid pipelines for leak and blockage detection. *Ph.D. thesis*, The Univ. of Adelaide, Adelaide, SA, Australia.

Lee, P.J., Vítkovský, J.P., Lambert, M.F., Simpson, A.R., and Liggett, J.A. (2003). Frequency response coding for the location of leaks in single pipeline systems. *The Int. Conference on Pumps, Electromechanical Devices and Systems Applied to Urban Water Management*, IAHR and IHRA, Valencia, Spain, April 22–25.

Lee, P.J., Vítkovský, J.P., Lambert, M.F., Simpson, A.R., and J.A. Liggett. (2005). Frequency domain analysis for detecting pipeline leaks. *J. Hydraulic Eng.* 131(7), 596-604.

Lee, P.J., Lambert, M.F., Simpson, A.R., Vítkovský, J.P., and Liggett, J. (2006). Experimental verification of the frequency response method for pipeline leak detection. *J. Hydraulic Res.* IAHR, 44(5), 693-707.

Lee, P.J., Duan, H.F., Ghidaoui, M.S., and Karney, B.W. (2013). Frequency domain analysis of pipe fluid transient behvaoirs. *J. Hydraulic Res.* IAHR, 51(6), 609-622.

Lee, P.J., Duan, H.F., Tuck, J., and Ghidaoui, M.S., (2015). Numerical and experimental study on the effect of signal bandwidth on pipe assessment using fluid transients. *J. Hydraulic Eng.* ASCE, 141(2), 04014074.

Liggett, J.A., and Chen, L.C. (1994). Inverse transient analysis in pipe networks. *J. Hydraulic Eng.* ASCE, 120(8), 934-954.

Meniconi, S., Brunone, B., Ferrante, M., and Massari, C. (2011). Potential of transient tests to diagnose real supply pipe systems: what can be done with a single extemporary test. *J. of Water Resources Planning and Management*, ASCE, 137(2), 238-241.

Meniconi S., Duan H.F., Lee PJ, Brunone B., Ghidaoui MS, and Ferrante M. (2013). Experimental Investigation of Coupled Frequency and Time-Domain Transient Test–Based Techniques for Partial Blockage Detection in Pipelines. *J. Hydraul. Eng.*, ASCE, 139(10), 10.1061/(ASCE)HY.1943-7900.0000768, 1033-1040.

Mpesha, W., Gassman, S. L., and Chaudhry, M. H. (2001). Leak detection in pipes by frequency response method. *J. Hydraulic Eng.* ASCE, 127(2), 134-147.

Nixon, W., Ghidaoui, M.S., and Kolyshkin, A.A. (2006). Range of validity of the transient damping leakage detection method. *J. Hydraulic Eng.* ASCE, 132(9), 944-957.

Sattar, A.M., and Chaudhry, M.H. (2008). Leak detection in pipelines by frequency response method. *J. Hydraulic Res.* IAHR, 46(EI1), 138-151.

Stephens, M (2008). Transient response analysis for fault detection and pipeline wall condition assessment in field water transmission and distribution pipelines. *PhD Thesis*, University of Adelaide, Australia.

Stephens, M., Lambert, M., Simpson, A., Vítkovský, J., and Nixon, J. (2004). Field tests for leakage, air pocket, and discrete blockage detection using inverse transient analysis in water distribution pipes. *World Water and Environmental Resources Congress*, ASCE, June 27-July 1, 2004, Salt Lake City, Utah, USA

Tang, K.W., Brunone, B., Karney, B., and Rossetti, A. (2000). Role and characterization of leaks under transient conditions. *Building Partnerships-Proc. ASCE Joint Conf. Water Resource Engineering and Management* Minneapolis MN, 7-30.

Vítkovský, J.P., Simpson, A.R., and Lambert, M.F. (2000). Leak detection and calibration using transients and genetic algorithms. *J. Water Res. Planning and Management*, ASCE, 126(4), 262-265.

Wang, X.J. (2002). Leakage and blockage detection in pipelines and pipe network systems using fluid transients. *PhD Thesis*. The University of Adelaide, Adelaide AU.

Wang, X.J., Lambert, M.F., Simpson, A.R., Liggett, J.A., and Vítkovský, J.P. (2002). Leak

detection in pipeline systems using the damping of fluid transients. *J. Hydraulic Eng.* ASCE, 128(7), 697-711.

Wylie, E.B., Streeter, V.L., and Suo, L.S. (1993). *Fluid transients in systems*. Prentice-Hall, Englewood Cliffs, New Jersey.